An Online $LiFePO_4$ Battery Impedance Estimation Method for Grid-tied Residential Energy Storage Systems

Andres Salazar, *Member, IEEE,* Carlos Restrepo, Yabiao Gao, Javad Mohammadpour Velni, *Member, IEEE,* Antonio Ginart, *Senior Member, IEEE.*

***Abstract*—There has recently been a significant interest directed towards residential battery storage systems mainly motivated by high penetration of renewables, the low cost and high efficiency of power electronic devices, and the advancements in the safety and energy density of the batteries, especially Lithium-Ion (Li-Ion) batteries. Furthermore, the possibility for the end user to become a utility-independent entity with the capacity to overcome power outages and tariff rises is even further propelling this fast growing industry. Lithium iron phosphate ($LiFePO_4$) battery is one of those technologies chosen to take the lead in residential battery storage due to its intrinsic safe performance, good energy density and price. This paper describes an online method for estimating the impedance of $LiFePO_4$ batteries when they are used in residential single phase energy storage systems. Single phase power systems have the intrinsic characteristics of delivering power at twice the frequency of the grid; by energy conservation principle, this pulsating characteristics is transferred directly to the current in the DC stage of the battery storage system. The proposed method takes advantage of this phenomenon and, without interrupting the energy conversion process or adding any external perturbation to the system, is able to characterize, in situ, the AC impedance behavior of the battery. Experimental results are provided to validate the proposed method and simulations show the potential applicability of this method in the assessment of the actual battery aging state.**

Keywords: ***Battery energy storage; Battery aging; Battery Impedance; DC/AC power conversion***

NOMENCLATURE

Z_{ac}	AC battery Impedance.
L_e	Battery parasitic inductance.
R_o	Battery ohmic resistance.
R_{ct}	Battery charge transfer resistance.
C_{dl}	Battery active layer capacitance.
Z_w	Battery Warburg impedance.
V_{DC}	Output DC voltage of battery.
I_{DC}	Output DC current of battery.
P_{DC}	Output DC power of battery.
V_{RMS}	Output RMS voltage of single phase inverter.
I_{RMS}	Output RMS current of single phase inverter.
P_{AC}	Output AC power of battery.
f_0	Fundamental grid voltage operating frequency.
$\hat{V}_{batt}$	Battery voltage AC component.
$\hat{I}_{batt}$	Battery current AC component.
η	Power conversion efficiency.
F_s	Sampling frequency.

A. Salazar, C. Restrepo and Y. Gao are with sonnen, Inc R&D, Atlanta, GA (e-mail: andres@sonnen-batterie.com)

J. Mohammadpour Velni is with the University of Georgia, Athens, GA (e-mail: javadm@uga.edu)

A. Ginart is with Smart Wires, Inc, San Francisco, CA (e-mail: antonio.ginart@smartwires.com)

I. INTRODUCTION

Residential AC nano-grids are playing an important role in the expandability of distributed renewable energy generation. These types of systems are generally composed of a Battery Energy Storage System (BESS), Photo-voltaic (PV) systems and interconnection and protection components (see Fig. 1). In recent years, BESSs have been fabricated using Lithium Ion (Li-Ion) batteries [1]. Li-Ion batteries can act in two ways; firstly as a buffer between the existing PV system installed in homes, accumulating the surplus of energy and minimizing the grid energy consumption, and secondly as a backup system, where in case of power grid outages the energy consumed by the home is provided by the batteries. In both cases, batteries interact with a sinusoidal power generation source through a power converter. In the residential US market, the power converters in charge of this interaction are single-phase DC/AC converters.

The performance of Li-Ion batteries changes based on different factors, such as temperature, capacity or state of charge

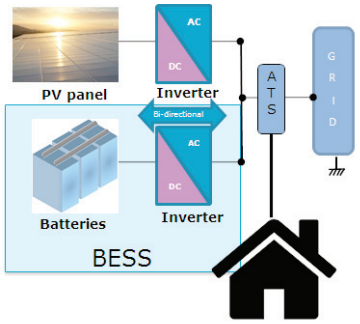

Fig. 1: Schematic of a typical AC nano-grid for residential applications.

(SOC), voltage and state of battery health (SOH) [2], [3]. Previous studies have shown the co-relation between the variation of the battery internal impedance and factors like SOC and battery aging or battery health degradation [2] -[4]. This last one is extremely important for dimensioning the economic impact over the investment of the systems, for preventing failures in the same and scheduled replacement of batteries.

One of the most common methods to measure the internal impedance of the Li-Ion batteries is the Electrochemical Impedance Spectroscopy (EIS) [2]. EIS is a very specialized technique and requires the use of laboratory equipment, which are sometimes expensive [5], and therefore not easy to implement in a Battery Management System (BMS). For this reason, low cost and online battery impedance measurement techniques for Li-Ion cells have been explored recently, especially by considering the interaction of the Li-Ion batteries with power electronic components. In [6], for instance, the authors propose the use of an excitation current generated by the PWM signals used in the motor control driver for Electric Vehicle (EV) applications. The latter paper concentrates on the estimation of the State of Charge (SOC) by means of the battery impedance. The method proposed in [7] uses a small duty-cycle sinusoidal perturbation in the gate drive signals of a DC converter located between a Li-Ion battery and a DC load. The voltage and current are measured to calculate the impedance of the cell at different frequencies. Finally, the authors in [8] extend the previous results by proposing a multiple frequency excitation by adding the sum of several sinusoidal functions and then measuring the battery and voltage spectrum.

The present paper introduces a novel online method to estimate a Li-Ion battery AC impedance at twice the fundamental grid frequency, without perturbing the power electronics control of the inverter used in AC nano-grid applications interacting with the AC power grid through single phase inverters. This method differentiates from those found in the literature, because those methods focus only on EVs and other DC applications where no interaction with AC sources is required. Furthermore, the above methods involve the use of a perturbation in the power electronics duty cycle, and hence modifying the closed-loop control of the power converters. The method proposed in this work essentially capitalizes on fundamental concepts associated with the energy transfer between Li-Ion batteries and single phase AC power sources. It will be shown how the intrinsic characteristics of these systems can help to determine, without the use of any external signal perturbation, the internal AC impedance for a specific frequency of operation. The paper develops an online method to extract the battery impedance information and tests it under real operating conditions. Finally, based on referenced aging data for $LiFePO_4$ batteries, this paper will show how to use the proposed method in order to develop an assessment over the life degradation of the battery.

II. Preliminaries and System Components

In this section, we describe various components involved in a grid-tied inverter and the associated analytical representation of the battery DC current and battery impedance.

A. Li-Ion Batteries Electrical Model

Fig. 2a illustrates a typical AC-impedance model for a Li-Ion battery. The components of this circuit are as follows: (1) parasitic inductor L_e, (2) ohmic resistance R_o, (3) charge transfer resistance R_{ct}, (4) double-layer capacitor C_{dl} as a result of activation polarization, and (5) Warburg impedance Z_w as a result of concentration polarization [10]. The battery AC-impedance Z_{ac} can then be expressed as follows

$$Z_{ac}(\omega) = jL_e\omega + R_o + (R_{ct} + Z_w)\|\frac{1}{jC_{dl}\omega}. \qquad (1)$$

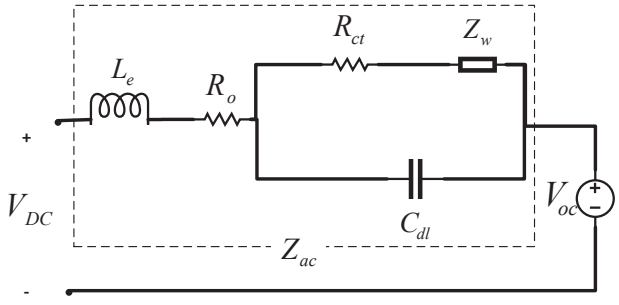

(a) Li-Ion cell electrical circuit representation.

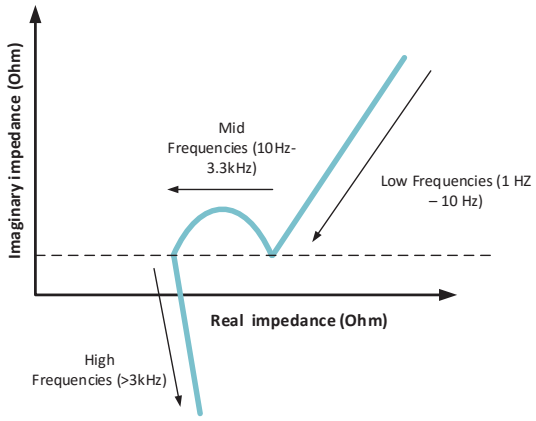

(b) Nyquist plot representation for the AC-battery impedance.

Fig. 2: Li-Ion battery model

A Nyquist plot for the battery impedance is shown in Fig. 2b. Normally this plot is obtained by Electrochemical Impedance Spectroscopy (EIS) analysis, measuring the phase displacement between current and voltage when an oscillatory current, at different frequencies, is injected to the battery. The parameters in (1) can be estimated by different techniques as shown in [2] and [11]. In the middle frequencies, the effect of the Warburg impedance and the inductance component are not that evident,

and hence for injected currents with frequencies in that range, the AC impedance can be modeled as

$$Z_{ac}(\omega) = R_o + (R_{ct} \| \frac{1}{jC_{dl}\omega}). \quad (2)$$

B. Power Conversion in Single Phase Inverters

A single phase power system experiences a pulsating power transfer between the batteries and the AC source that can be computed based on the energy conservation principle as

$$P_{DC} = I_{DC}V_{DC} = \eta I_{RMS}V_{RMS} = P_{AC}. \quad (3)$$

Assuming that the efficiency η and the power factor are equal to one, the instantaneous values for the current and voltage are obtained from (4), where $\omega_0 = 2\pi f_0$ and f_0 is the fundamental frequency of the power grid [12].

$$\begin{aligned} V_{DC}I_{DC} &= \sqrt{2}V_{RMS}sin(\omega_0 t)\sqrt{2}I_{RMS}sin(\omega_0 t) \\ &= 2V_{RMS}I_{RMS}sin^2(\omega t). \end{aligned} \quad (4)$$

As a result, the battery DC current should have a quadratic sine form as shown in (5) and (6). A plot of $I_{DC}(t)$ is shown in Fig. 3b.

$$I_{DC}(t) = \frac{2V_{RMS}I_{RMS}sin^2(\omega_0 t)}{V_{DC}}. \quad (5)$$

Assuming no losses in the power conversion process, the battery DC current can be rewritten as

$$I_{DC}(t) = 2I_{DC}sin^2(\omega_0 t). \quad (6)$$

This leads to the conclusion that the current waveform flowing through the battery in a DC/AC energy conversion process is alternating at twice the frequency of the fundamental grid frequency, and hence

$$\begin{aligned} I_{DC}(t) &= I_{DC}(1 + cos(2\omega_0 t)) \\ &= I_{DC} + \hat{I}_{batt}(t), \end{aligned} \quad (7)$$

where $\hat{I}_{batt}(t)$ is the AC component of the battery current. Fig. 3c depicts the actual measurement of the battery current and voltage during the DC/AC power conversion that demonstrates the quadratic sine wave form of the current and also its influence over the DC voltage, where a ripple oscillation with the same frequency of the current is present. It is clear then that both measurements have a DC component and AC components.

III. Description of the Proposed Method for Estimating the Internal Battery Impedance

Equation (8) below is utilized to represent the transfer function of the AC battery impedance derived from (2).

$$Z_{ac}(s) = \frac{s^2R_aC_{dl} + s(R_oR_aC_{dl}) + R_o + R_a}{sR_aC_{dl} + 1}. \quad (8)$$

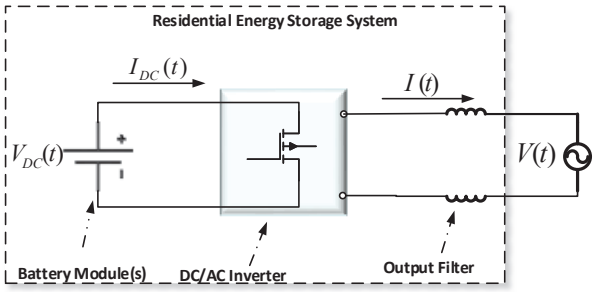

(a) Power conversion in a battery energy storage system.

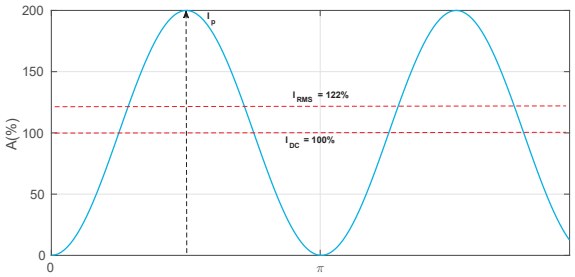

(b) Battery current shape during the power conversion process.

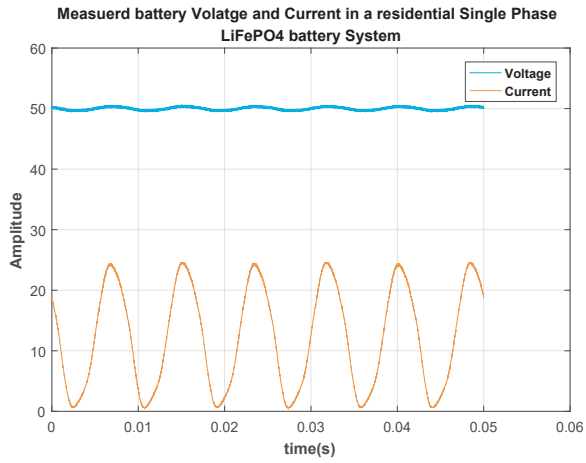

(c) Battery current and voltage during the power conversion.

Fig. 3: Battery current and voltage waveforms during power conversion process (DC/AC - AC/DC) using a single phase inverter.

During the DC/AC power conversion process, the battery's over potential voltage (V_{op}) at twice the grid frequency can be obtained by combining (8) and (7) as

$$V_{op} \equiv |Z_{ac}(2\omega_o)|\, I_{DC}cos(2\omega_o t + \angle Z_{ac}(2\omega_o)), \quad (9)$$

where $\omega_o = 2\pi f_o$ and f_o is the frequency of the power grid.

The AC part of (9) represents the voltage ripple caused by the oscillatory behavior of the current at $2f_o$. It is possible to

approximate the AC component of the voltage in the battery terminals to V_{op}, i.e., $\hat{V}_{batt} \equiv \hat{V}_{op}$. Then, the AC battery impedance at the frequency $2f_o$ can be expressed as

$$|Z_{ac}(2\omega_o)| = \frac{\mathscr{F}\{\hat{V}_{batt}(t)\}}{\mathscr{F}\{I_{DC}cos(2\omega_o t + \angle Z(2\omega_o))\}}. \quad (10)$$

This shows that by only measuring the current flowing into the battery and the voltage in the battery terminals, an estimation of the internal AC impedance of the cells, for a specific grid frequency, can be achieved.

Online Battery Impedance Estimation

The proposed online method for battery impedance estimation consists of sampling the voltage $V_{DC}(t)$ and current $I_{DC}(t)$ at the battery terminals, and then, obtaining the high frequency components by removing the DC components using a moving average filter. The difference equation (11) shows the recursive representation of this filter.

$$y(k) = ax(k) + y(k-1) + bx(k-N), \quad (11)$$

where $a = 1/N$, $b = -1/N$ and N is the number of samples. For the initialization of this filter, i.e., $k = 1$, it is required to store N elements in order to calculate $y(0) = M$, where M is determined by averaging the stored N samples as

$$M = \frac{1}{N}\sum_{k=1}^{N} x(k).$$

Then, the filtered signal is passed through a second order Goertzel filter, which will allow the extraction of the signal magnitude at the desired frequency [13]. The transfer function of this filter is given by

$$H(z) = \frac{v(z)}{y(z)} = \frac{1 - w_N^{-\frac{2f_0 N}{F_s}} z^{-1}}{1 - (2cos(\frac{4\pi f_0}{F_s}))z^{-1} + z^{-2}}, \quad (12)$$

where F_s is the sampling frequency. With N samples, the filter output will give the signal Fourier transform at the frequency $2f_0$ as

$$\hat{V}(2fo) = cos(\frac{4\pi f_0}{F_s})v(N-1) - v(N-2) + jsin(\frac{4\pi f_0}{F_s})v(N-1). \quad (13)$$

Finally the impedance of the battery at twice the grid frequency is obtained by dividing the real part of the processed battery voltage $\hat{V}_{batt}$ and battery current $\hat{I}_{batt}$ as

$$Z_{ac}(2f_0) = \frac{\Re(\hat{V}_{batt}(2fo))}{\Re(\hat{I}_{batt}(2fo))}. \quad (14)$$

IV. Implementation of the Proposed Method

The method described in the previous section is implemented in the main microprocessor of the DC/AC power converter as shown in Fig. 4. Fig. 5 depicts the block diagram for the different modules to be implemented in the firmware application. Different interrupt subroutines (ISR) levels are highlighted in the diagram, where ISR_0 indicates the highest priority ISR.

The batteries used for the testing purposes are a commercial type of $LiFePO_4$. They are enclosed in a module under a series and parallel arrangement with a capacity of 2kWh. The AC impedance (per data sheet) is $35m\Omega$ or less. A lab prototype bidirectional inverter of 4kW output is used for obtaining the initial results with main grid frequency of 60Hz, i.e., $f_o = 60Hz$. Estimation of the battery impedance is done at different SOC (State of Charge) levels, going from 7% to 75%. The battery charge and discharge is done continuously at approximately $0.35C$, where C is the rate of charge or discharge relative to the capacity of the battery. In this case, $1C$ means that at the rated current, the batteries are discharged or charged in 1 hour. The maximum temperature of the battery module is also monitored with the BMS provided by the manufacturer. Fig 6b shows the current flowing into the batteries and the battery voltage AC component while the charging process takes place.

The continuous current flowing during the entire testing process increases the internal cell temperature but the external temperature is kept constant at $25°C$. This temperature increase was considered during the experiments and three scenarios were studied. The first is when the internal average temperature of the cells was $30.57°C$, the second is when the temperature was $37.29°C$, and the last one is for an average internal temperature of $39°C$. The same scenarios are run several times and the mean value (μ) of the calculated impedance is summarized in Table I. This table also shows the variance (σ), and the coefficient of variation ($c_v = \sigma/\mu$) for the analyzed data.

$Z(f_o)$	$T = 30.57°C$	$T = 37.29°C$	$T = 39.02°C$
μ	$28.8m\Omega$	$27.2m\Omega$	$26.8m\Omega$
σ	2.81×10^{-7}	9.45×10^{-8}	3.20×10^{-8}
c_v	9.82×10^{-6}	3.47×10^{-6}	1.18×10^{-6}

TABLE I: Calculated impedances for different SOC and different internal battery temperatures.

Fig. 7 illustrates the magnitude of the FFT for one of the mentioned scenarios. A variability in the obtained voltage and current is observed for different SOC levels, which led to variations in the calculated impedance value. However, from the analysis presented in Table I, it can be inferred that the calculated impedance may be considered constant during the entire charge or discharge process and the SOC does not affect the AC impedance calculation at this frequency, which is consistent with the results obtained for a different type of $LiFePO_4$ batteries in [2] and [3]. Furthermore, the observed dependency on the internal cell temperature is also consistent with the results presented in [3], where spectroscopy analysis results are presented at different temperatures.

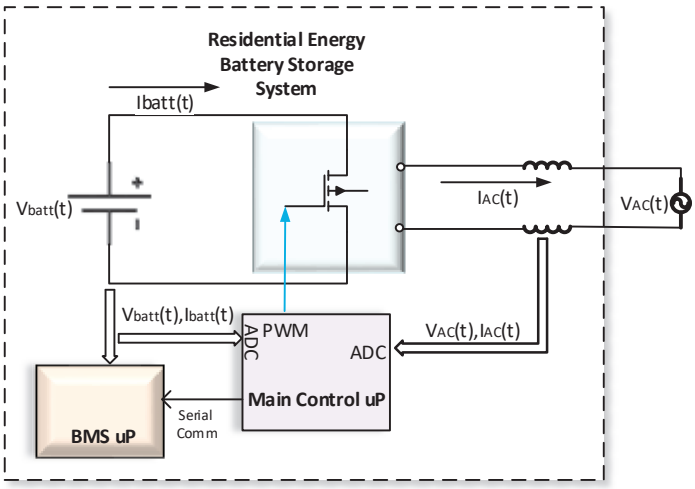

Fig. 4: Implementation of the proposed method.

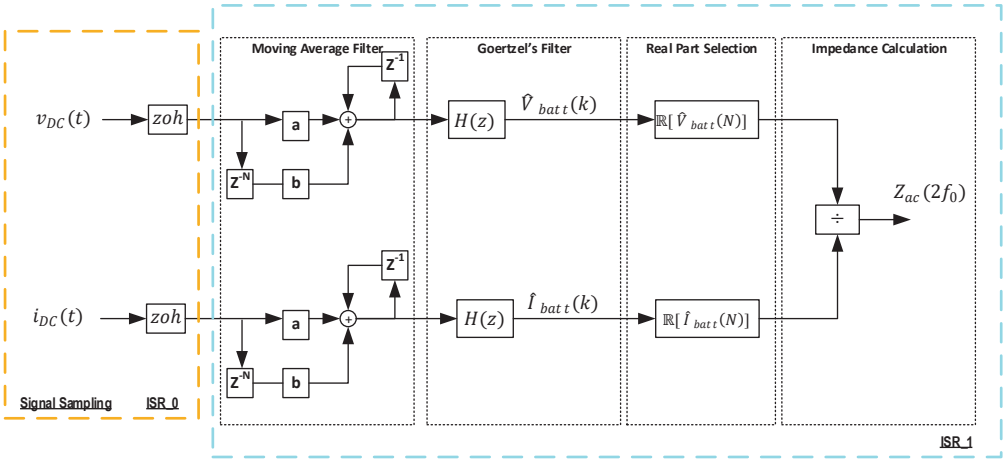

Fig. 5: Block Diagram representation for implementation of the proposed method.

V. Towards Battery Aging Diagnostic

It has been shown in previous studies that the real (or ohmic) part of the battery increases with the increase of battery life cycles [2], [3], [14]. Fig. 8 shows a typical Nyquist plot of a Li-Ion battery at the beginning of and end of its life. Therefore, it is possible to examine the battery lifetime by measuring the battery impedance.

We have introduced the battery model parameters described in previous sections to a simulation model of a commercial split phase bi-directional converter, where the proposed method is implemented in parallel with the control model. The parameters, for a specific type of $LiFePO_4$ battery, have been extracted from [2] and are presented in Table II. Table III shows the results of the estimated impedance using the proposed method of this paper. It can be observed that by using the proposed method, the same percentage of increase can be inferred as that measured by [2] at different battery life cycles. This could help in developing an online detection scheme over the lifetime of the battery.

Cycles	R_o	R_{ct}	C_{dl}	L_e
0 Cycles	$5.1m\Omega$	$80m\Omega$	680F	$18.84mH$
7600 Cycles	$5.5m\Omega$	$140m\Omega$	550F	$18.84mH$

TABLE II: Simulation results used for battery life diagnostic.

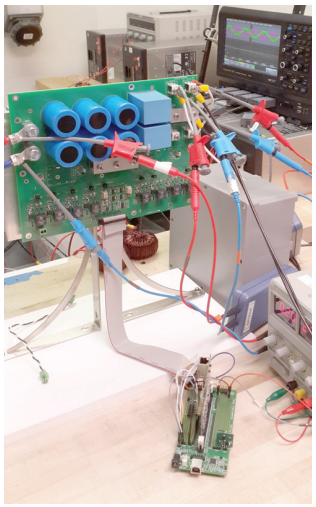

(a) Experimental setup.

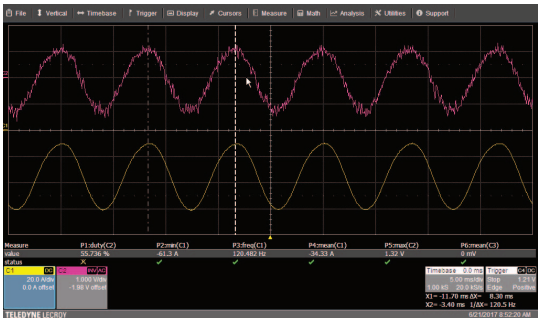

(b) Battery current (C1-Yellow) and AC component of battery voltage (C2-Magenta).

Fig. 6: Implementation of the proposed impedance estimation method.

Cycles	Estimated $Z(2f_0)$
0 Cycles	$5.0925m\Omega$
7,600 Cycles	$5.518m\Omega$
Estimated increase	8.3%
Measured increase	7.8%

TABLE III: Results achieved by the proposed method.

VI. Conclusions

This paper has examined the power conversion process in a single phase residential battery storage system. It is demonstrated that the pulsating power transfer characteristics in these systems leads to a quadratic sinusoidal current waveform flowing through the Li-Ion batteries, where the fundamental frequency of the AC component of the battery current is twice the power grid frequency. By having this information, we have shown how to obtain an expression for the estimation of the AC battery impedance at this frequency. The implementation of the proposed methodology for online estimation of

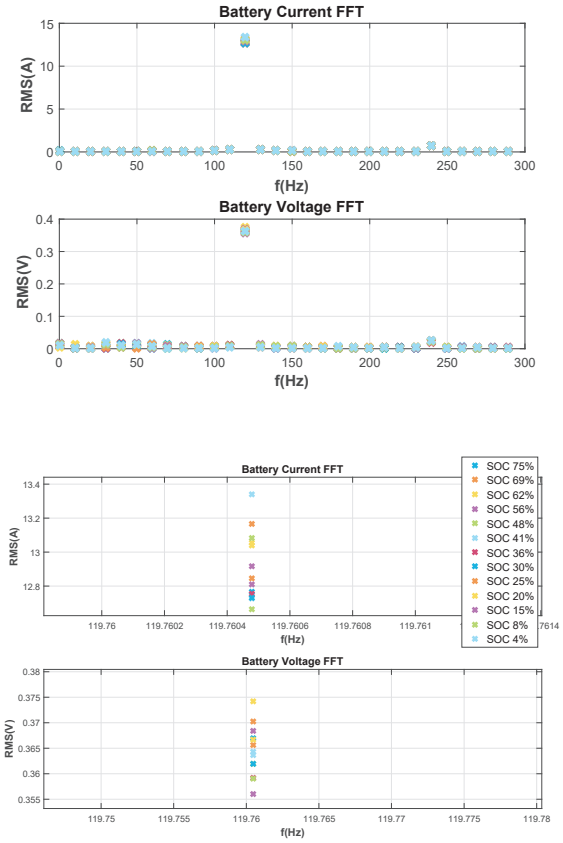

Fig. 7: FFT of the battery voltage and current at average internal cell temperature of $30°C$

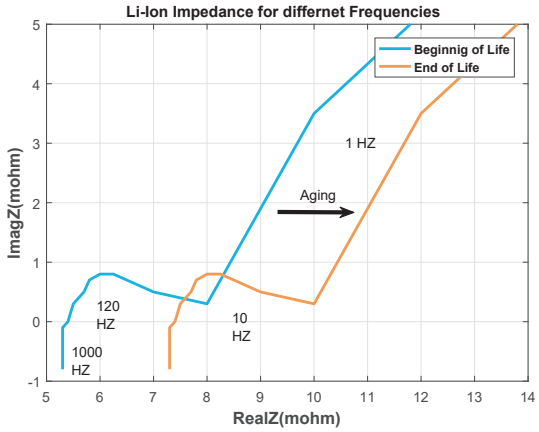

Fig. 8: AC-battery impedance before and after aging.

the battery impedance is described with the presented results supporting the accuracy and reliability of the proposed method. The proposed method can further allow the online assessment of the health degradation of Li-Ion battery impedance, and hence constitutes the first step in the analysis of online SOH

estimation of Li-Ion batteries when they are used in residential single phase applications. Our current studies focus on the aging feature extraction.

REFERENCES

[1] C. Restrepo, A. Salazar, H. Schweizer, and A. Ginart, "Residential battery storage: Is the timing right?" *IEEE Electrification Magazine*, vol. 3, no. 3, pp. 14–21, Sept 2015.

[2] D. I. Stroe, M. Swierczynski, A. I. Stan, V. Knap, R. Teodorescu, and S. J. Andreasen, "Diagnosis of lithium-ion batteries state-of-health based on electrochemical impedance spectroscopy technique," in *2014 IEEE Energy Conversion Congress and Exposition (ECCE)*, Sept 2014, pp. 4576–4582.

[3] M. wierczyski, D. I. Stroe, A. I. Stan, R. Teodorescu, and D. U. Sauer, "Selection and performance-degradation modeling of $limo_2/li_4ti_5o_{12}$ and $lifepo_4/c$ battery cells as suitable energy storage systems for grid integration with wind power plants: An example for the primary frequency regulation service," *IEEE Transactions on Sustainable Energy*, vol. 5, no. 1, pp. 90–101, Jan 2014.

[4] J. Vetter, P. Novak, M. R. Wagner, C. Veit, K.-C. Moller, J. O. Besenhard, M. Winter, M. Wohlfahrt-Mehrens, C. Vogler, and A. Hammouche., "Aging mechanism in lithium-ion batteries," *Journal of Power Sources*, no. 147, pp. 269–281, 2005.

[5] L. Lu, X. Han, J. Li, J. Hua, and M. Ouyang, "A review on the key issues for lithium-ion battery management in electric vehicles," *Journal of Power Sources*, vol. 226, pp. 272 – 288, 2013.

[6] D. A. Howey, P. D. Mitcheson, V. Yufit, G. J. Offer, and N. P. Brandon, "Online measurement of battery impedance using motor controller excitation," *IEEE Transactions on Vehicular Technology*, vol. 63, no. 6, pp. 2557–2566, July 2014.

[7] W. Huang and J. A. A. Qahouq, "An online battery impedance measurement method using DC/DC power converter control," *IEEE Transactions on Industrial Electronics*, no. 11, pp. 5987–5995, 2014.

[8] J. A. A. Qahouq, "Online battery impedance spectrum measurement method," in *2016 IEEE Applied Power Electronics Conference and Exposition (APEC)*, March 2016, pp. 3611–3615.

[9] J. Yu, "Health degradation detection and monitoring of lithium-ion battery based on adaptive learning method," *IEEE Transactions on Instrumentation and Measurement*, vol. 63, no. 7, pp. 1709–1721, July 2014.

[10] S. Y. Cho, I. O. Lee, J. I. Baek, and G. W. Moon, "Battery impedance analysis considering DC component in sinusoidal ripple-current charging," *IEEE Transactions on Industrial Electronics*, vol. 63, no. 3, pp. 1561–1573, March 2016.

[11] X. Tang, X. Mao, J. Lin, and B. Koch, "Li-ion battery parameter estimation for state of charge," in *Proceedings of the 2011 American Control Conference*, June 2011, pp. 941–946.

[12] A. Ginart, A. Salazar, and R. Liou, "Transformerless bidirectional inverter for residential battery storage systems," in *2016 IEEE Green Technologies Conference (GreenTech)*, April 2016, pp. 18–23.

[13] M. A. Jaber and D. Massicotte, "Fast method to detect specific frequencies in monitored signal," in *2010 4th International Symposium on Communications, Control and Signal Processing (ISCCSP)*, March 2010, pp. 1–5.

[14] M. V. Micea, L. Ungurean, G. N. Carstoiu, and V. Groza, "Online state-of-health assessment for battery management systems," *IEEE Transactions on Instrumentation and Measurement*, vol. 60, no. 6, pp. 1997–2006, June 2011.